Optical Characterisation of a Three Layer Waveguide Structure by m-Lines Spectroscopy

Thomas Schneider, Dominique Leduc, Julien Cardin, Cyril Lupi, Hartmut Gundel

Optical Characterisation of a Three Layer Waveguide Structure by m-Lines Spectroscopy

T. SCHNEIDER, D. LEDUC, J. CARDIN, C. LUPI, AND H. GUNDEL

Université de Nantes, Nantes Atlantique Universités, IREENA, EA 1770, Faculté des Sciences et des Techniques, 2 rue de la Houssinière - BP 9208, Nantes, F-44000 France

A three layer planar waveguide structure, consisting of a light guiding ferroelectric lead zirconate titanate thin film, embedded between two transparent zinc oxide electrodes, was elaborated and studied by m-lines spectroscopy. The three layer modal dispersion equations are established and we demonstrate experimentally the ability to retrieve the refraction index and the thickness of each individual layer of the composite waveguide from one single m-lines spectroscopy measurement.

Keywords M-lines spectroscopy; composite waveguide; PZT; ZnO; thin film

Introduction

Ferroelectric thin films may exhibit interesting optical properties, such as large electro-optic effects (Pockels, Kerr), a high refraction index, and a high transparency at visible and infra red wavelengths. These properties are promising for the realization of many applications in the field of integrated optics, like for sensors or for optical communication components (optical shutters, waveguides, filters, etc.). In order to obtain active devices, which profit from the electro-optic properties of these materials, electrodes have to be integrated. They can be either metallic [1] or may consist of transparent conductive material like indium tin oxide (ITO) or aluminium doped zinc oxide (ZnO) in the case where the absorption of light is a critical factor. The design of such components requires an accurate characterization of the optical properties of each layer. M-lines spectroscopy [2–4] is known to be very efficient for the characterisation of single layer films. The case of multilayer guides, however, is less investigated. Only few studies of two layer structures were performed [5–9] and investigation of three layer waveguides is not yet reported. The aim of the present paper is to generalize the use of the m-lines spectroscopy for the characterization of these structures.

The first part of this paper is devoted to the development of the modal dispersion equations for a three layer waveguide where the central layer has a higher refractive index as the confining gain layers. To the best of our knowledge, these equations have not yet been reported elsewhere. In the second part, the elaboration of the waveguide is described,

the structure is analysed step by step by m-lines spectroscopy, and finally an experimental characterization of a three layer waveguide is presented.

The Two and Three Layer Dispersion Equations

The m-lines device is the classical setup where the light of a HeNe laser is focused on the base of a prism, which is pressed against the film. The prism and the film are mounted on a rotating stage in order to allow a variation of the angle of incidence. The incident light is totally reflected by the prism-film interface, except for the synchronous angles where part of the light is coupled into the film. The synchronous angles are given by the dispersion equation of the planar waveguide. Hence, the analysis of the m-lines spectra requires knowing the dispersion equation of the studied guide (in the present case we shall consider only the TE modes). Due to its compactness, the transfert matrix method [10] is well suited for analysing multilayer waveguides, the geometry which is shown in Fig. 1. The layer j has a refraction index n_j and a thickness d_j. The layer 0 represents the substrate and the layer 4 the superstratum. In our case, $n_0 = 1.5169$ and $n_4 = 1$ at 632.8 nm wavelength. For the TE modes, the electrical field in the layer j has only one component along the (Oy) axis $E_{jy}(x, z) = A_j e^{i\gamma x} e^{i\beta_m z} + B_j e^{-i\gamma x} e^{i\beta_m z}$ and the tangential component of the magnetic field is $H_{jz} = i(\omega\mu_0)^{-1} \mathrm{d}E_{jy}/\mathrm{d}x$. In these expressions, ω is the angular frequency, γ_j is the x-component of the wave vector $\gamma_j = i[(n_j k)^2 - \beta_m^2]^{1/2}$, where n_j is the refractive index of the layer and β_m is the propagation constant of the mth guided mode, which is usually written as $\beta_m = kN_m$, where $k$is the wave vector modulus in vacuum and N_m the effective index. The term γ_j gives the nature of the waves in the layer j which is real in the case of travelling waves and purely imaginary in the case of evanescent waves. To each layer, a transfer matrix M_j will be associated [10]:

$$M_j = \begin{pmatrix} \cos\gamma_j d_j & \dfrac{i}{\gamma_j}\sin\gamma_j d_j \\ i\gamma_j \sin\gamma_j d_j & \cos\gamma_j d_j \end{pmatrix} \tag{1}$$

In order to satisfy the boundary conditions, the tangential component of the electric and the magnetic fields E_y and H_z have to be continuous at the interface of the layers. Together

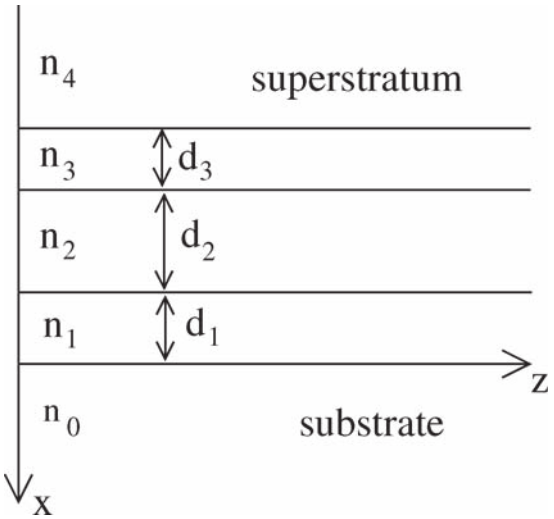

Figure 1. Three layer waveguide.

with the condition for light guiding, this leads to the equation

$$\begin{pmatrix} 1 \\ -\gamma_4 \end{pmatrix} E_{0y} = M_3 M_2 M_1 \begin{pmatrix} 1 \\ \gamma_0 \end{pmatrix} E_{0y} = M \begin{pmatrix} 1 \\ \gamma_0 \end{pmatrix} E_{0y} \tag{2}$$

that has solutions only when

$$\gamma_4 m_{11} + \gamma_4 \gamma_0 m_{12} + m_{21} + \gamma_0 m_{22} = 0 \tag{3}$$

with m_{ij} being the components of the matrix M. Inserting the values of m_{ij} given by equations (1) and (2) into (3) and assuming that $n_2 > n_1, n_3$ due to the fact that the refractive index of the central layer was supposed to be higher than that of the optical gain layers, we find after some algebric computation that the dispersion equation of the three layer waveguide can be written in the general form:

$$a_2 d_2 - \arctan\left[\frac{a_0\gamma_1 - \gamma_1^2 \tan(\gamma_1 d_1)}{\gamma_1 a_2 + a_0 a_2 \tan(\gamma_1 d_1)}\right] - \arctan\left[\frac{a_4\gamma_3 - \gamma_3^2 \tan(\gamma_3 d_3)}{\gamma_3 a_2 + a_4 a_2 \tan(\gamma_3 d_3)}\right] - m\pi = 0 \tag{4}$$

where $a_j = k|n_j^2 - N_m^2|^{1/2}$. At first glance, equation (4) may appear similar to the dispersion equation of a single layer guide. Depending on the terms γ_1 and γ_3 which may be imaginary or real, however, the waves in layer 1 and layer 3 become evanescent or travelling, respectively. Thus equation (4) comprises in fact four different dispersion equations also including information on the respective guiding conditions. In the case where $n_2 > n_3 > n_1$, three possibilities of wave guiding exist, which is shown in Fig. 2. The lowest order modes are exclusively confined in layer 2 (Fig. 2a), γ_1 and γ_3 become imaginary, thus explaining the change from the function *tangent* to the function *hyperbolic tangent* in the argument of the functions *arctangent*. Intermediate modes correspond to propagation in two layers. Guiding in layer 2 and 3 is obtained when $n_3 > n_1$ (Fig. 2b), propagation in layer 2 and 1 exists when $n_1 > n_3$ (not shown in Fig. 2). Finally, highest order modes propagate in the whole structure (Fig. 2c).

The dispersion equations for a two layer waveguide [11] can be easily deduced from the dispersion equation for the three layer waveguide in the limit $d_3 \to 0$:

$$a_2 d_2 - \arctan\left[\frac{a_0\gamma_1 - \gamma_1^2 \tan(\gamma_1 d_1)}{\gamma_1 a_2 + a_0 a_2 \tan(\gamma_1 d_1)}\right] - \arctan\left(\frac{a_4}{a_2}\right) - m\pi = 0 \tag{5}$$

In this case, two guiding regimes are possible: the lower order modes are confined in layer 2 while the higher order modes are guided by both layers.

Characterization of a three layer waveguide requires determining seven unknowns, the refractive indexes and thicknesses of the three layers and the order m_1 of the first mode appearing in the m-lines spectrum. Very often, the first mode in the spectrum is assumed to be the fundamental mode. The low order modes, however, are difficult to excite since they require large angles of incidence and hence spectra without the fundamental mode are often observed. Therefore, we do not make any assumption on the order of the first mode and shall consider it as an unknown. As a consequence, at least seven modes have to be identified in the m-lines spectrum in order to determine all unknowns. In general, *i.e.* when the thicknesses of the layers and the differences between the refractive indexes are large enough, a spectrum contains $M > 7$ modes. The order of the first mode propagating in 2 layers (m_2) and the order of the first mode propagating in 3 layers (m_3) have also to be determined.

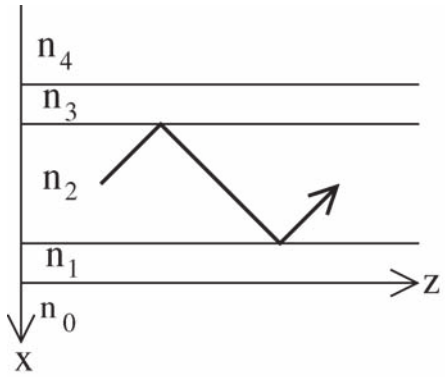

Dispersion equation

$$a_2\,d_2 \;-\arctan\left[\frac{a_0\,a_1+a_1^2\tanh(a_1\,d_1)}{a_1\,a_2+a_0\,a_2\tanh(a_1\,d_1)}\right] -\arctan\left[\frac{a_3\,a_4+a_3^2\tanh(a_3\,d_3)}{a_2\,a_3+a_2\,a_4\tanh(a_3\,d_3)}\right]-\;m\,\pi=0$$

a)

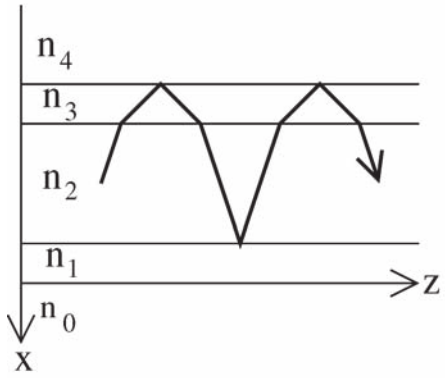

Dispersion equation

$$a_2\,d_2 \;-\arctan\left[\frac{a_0\,a_1+a_1^2\tanh(a_1\,d_1)}{a_1\,a_2+a_0\,a_2\tanh(a_1\,d_1)}\right] -\arctan\left[\frac{a_3\,a_4-a_3^2\tan(a_3\,d_3)}{a_2\,a_3+a_2\,a_4\tan(a_3\,d_3)}\right]-\;m\,\pi=0$$

b)

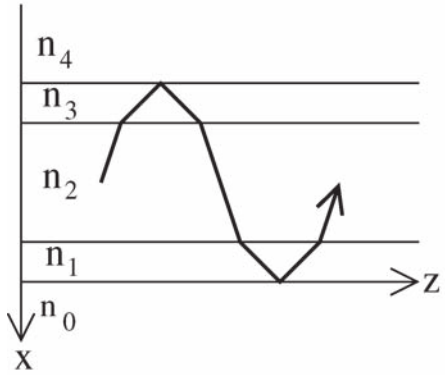

Dispersion equation

$$a_2\,d_2 \;-\arctan\left[\frac{a_0\,a_1-a_1^2\tan(a_1\,d_1)}{a_1\,a_2+a_0\,a_2\tan(a_1\,d_1)}\right] -\arctan\left[\frac{a_3\,a_4-a_3^2\tan(a_3\,d_3)}{a_2\,a_3+a_2\,a_4\tan(a_3\,d_3)}\right]-\;m\,\pi=0$$

c)

Figure 2. Wave guiding in one layer (a), two layers (b) and three layers (c) in the case of a three layer film where $n_2 > n_3 > n_1$.

In order to retrieve the thin films characteristics, we consider the six unknowns $\{n_j, d_j\}_{j=1,2,3}$ and we varie m_1 from one to M and m_2 and m_3 are iterated from $m_1 + 1$ to M. The C_M^6 systems of the six dispersion equations of type (4) are solved with a Newton-Raphson algorithm. For each value of m_1, we obtain $C \leq C_M^6$ sets of solutions. The synchronous angles ϕ_{cal} corresponding to each solution are calculated with a bisection algorithm and we compute the mean difference between these angles and the measured synchronous angles ϕ_{meas}: $\sigma(m_1, m_2, m_3) = [\sum_{i=1}^{C} \sum_{j=0}^{M-1} (\phi_{ij}^{\text{cal}} - \phi_j^{\text{meas}})^2 / MC^2]^{1/2}$. The minimum of the $\sigma(m_1, m_2, m_3)$ function gives the correct indexation. Finally, the solution is the mean value of the solutions corresponding to the correct indexation.

In order to characterize the two layer waveguides, a similar method is used, however, equation (4) has been replaced by equation (5).

Experimental Results

In order to verify the three layer model and the corresponding solution algorithm, two and three layer composite wave guides were elaborated on glass substrates, based on the use of

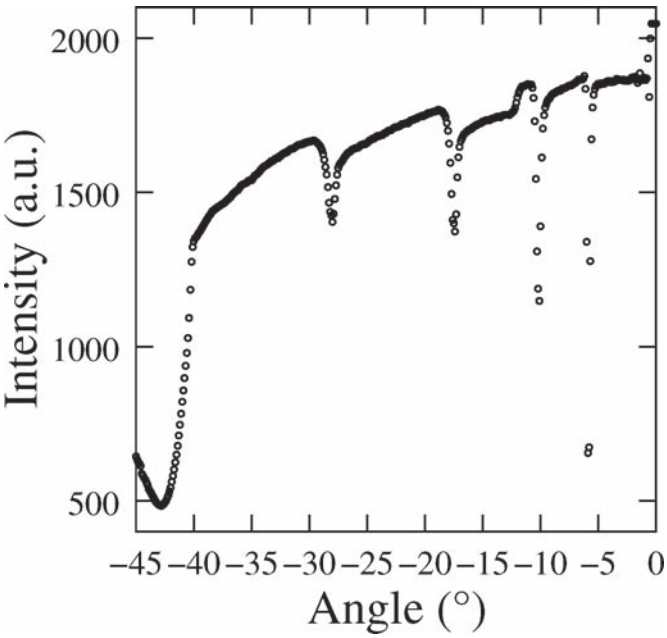

Figure 3. M-lines spectrum of a ZnO film.

lead zirconate titanate (PZT) as a light guiding layer (n_2 and d_2, cf. Fig. 1) and transparent, conducting Al doped zinc oxide (ZnO) for the optical gain (n_1, n_3, d_1 and d_3).

The zinc oxide layers were grown by RF magnetron sputtering at room temperature from a 3″ in diameter ZnO/Al_2O_3 (98/2 wt.%) ceramic target. Prior to the deposition, a pressure lower than $5.10^{-7} mbar$ was reached and pure argon was used as a sputter gas at a partial pressure of 2.10^{-3} *mbar* during the deposition process. An on-axis growth rate of approximately 100 nm/min was achieved at a RF power of 200 W at a target-substrate distance of 7.5 cm. As several samples were grown at the same time, the substrates had to be shifted off-axis, resulting in a non-homogeneous thickness of the ZnO film. The films were annealed at 650°C during 3 min and cooled down to room temperature during 3 hours.

M-lines measurements were taken at several points of the samples at 5 mm spacing. An example of the spectra is shown in Fig. 3 where five modes can be seen. The evolution of the refraction index and the thickness of the film as a function of the distance from the deposition center are represented in Fig. 4. The thickness of the ZnO layer decreases from 1.04 μm to 0.54 μm while the refraction index varies only slightly between 1.975 ± 5.10^{-3} and 1.964 ± 1.10^{-3}. Similar results were found for the other samples.

In order to establish a two layer waveguide, PZT 36/64 thin films were elaborated by Chemical Solution Deposition technique. A modified Sol-gel process was used for the elaboration of the PZT precursor solution, which consisted of lead acetate dissolved in acetic acid, zirconium and titanium n-propoxide; ethylene glycol was added in order to prevent from crack formation during the annealing process [12]. The final solution was spin-coated on the ZnO layer at 1000 rpm and the deposited films were dried on a hot plate. A Rapid Thermal Annealing procedure at 650°C resulted in the formation of a polycrystalline perovskite without remaining pyrochlore phases.

The PZT/ZnO films were characterised by m-lines spectroscopy at several points, an example of which is shown in Fig. 5. The narrow peaks at the left hand side of the spectrum correspond to the wave guiding in both layers while the broad peaks at positive angles correspond to wave guiding in the PZT layer only. The broadening of the peaks does not represent a peculiarity of the two layer structure; it is also observed when characterising

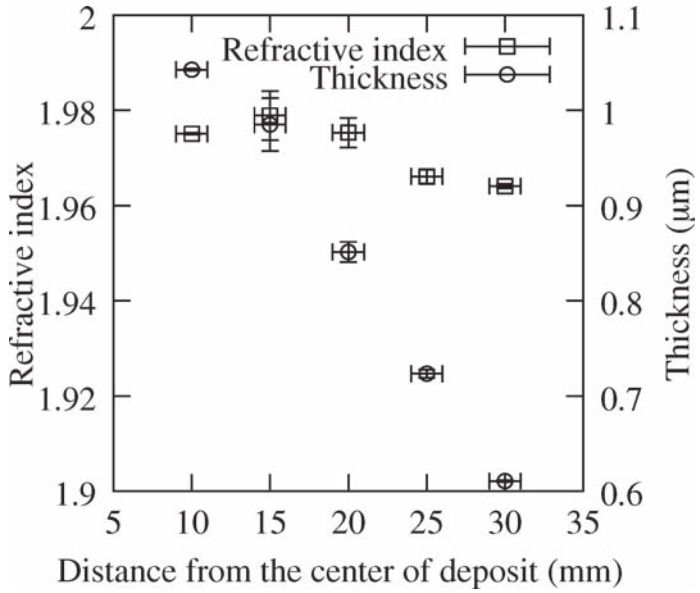

Figure 4. Evolution of the refraction index and the film thickness of a ZnO layer.

a PZT monolayer and is probably due to light diffusion as a consequence of the ceramic character of the PZT thin film.

For the analysis of the spectra, only the modes 4 to 8 (at negative angles) were considered which can be located with a precision of $\pm$ 0.05°, while the uncertainty on the position of the first modes is of the order of 0.1° due to of the broadening of the peaks. From this measurement the uncertainties on the refraction indexes $\Delta n_1 = \pm 3.10^{-3}$ and $\Delta n_2 = \pm 3.10^{-4}$ and on the thickness $\Delta d_1 = \pm 1.10^{-2}$ μm and $\Delta d_2 = \pm 3.10^{-3}$ μm were obtained for the ZnO and the PZT film, respectively. The results obtained as a function of the distance from the deposition center are shown in Fig. 6. A good agreement between the measurements from the single and the double layer structure for the refraction index and the thickness of the ZnO layer can be seen. The difference is of the order of 10^{-2} for the refraction index and 100 nm for the thickness in the worst case, however, remains in general below the uncertainty of the measurement.

The measurement of the PZT refraction index reveals the influence of the ZnO interface between the PZT and the substrate on the crystallisation behaviour of the ferroelectric. A

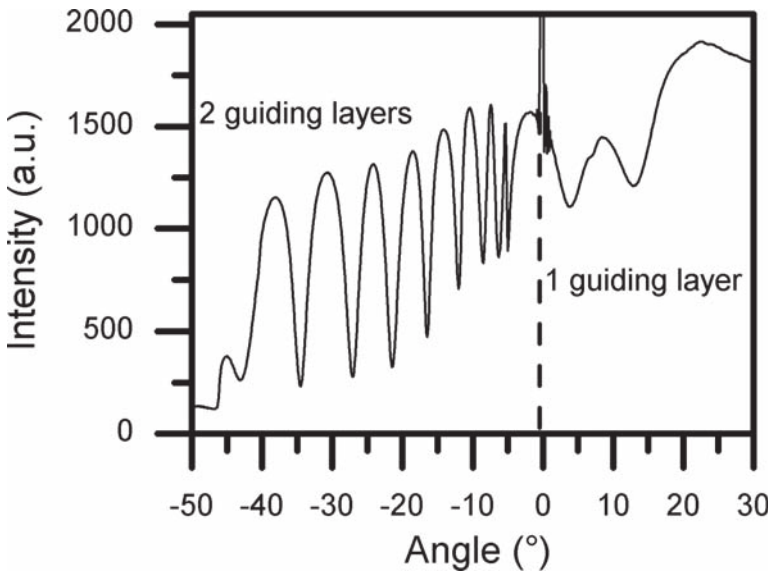

Figure 5. M-lines spectrum of a two layer PZT/ZnO structure.

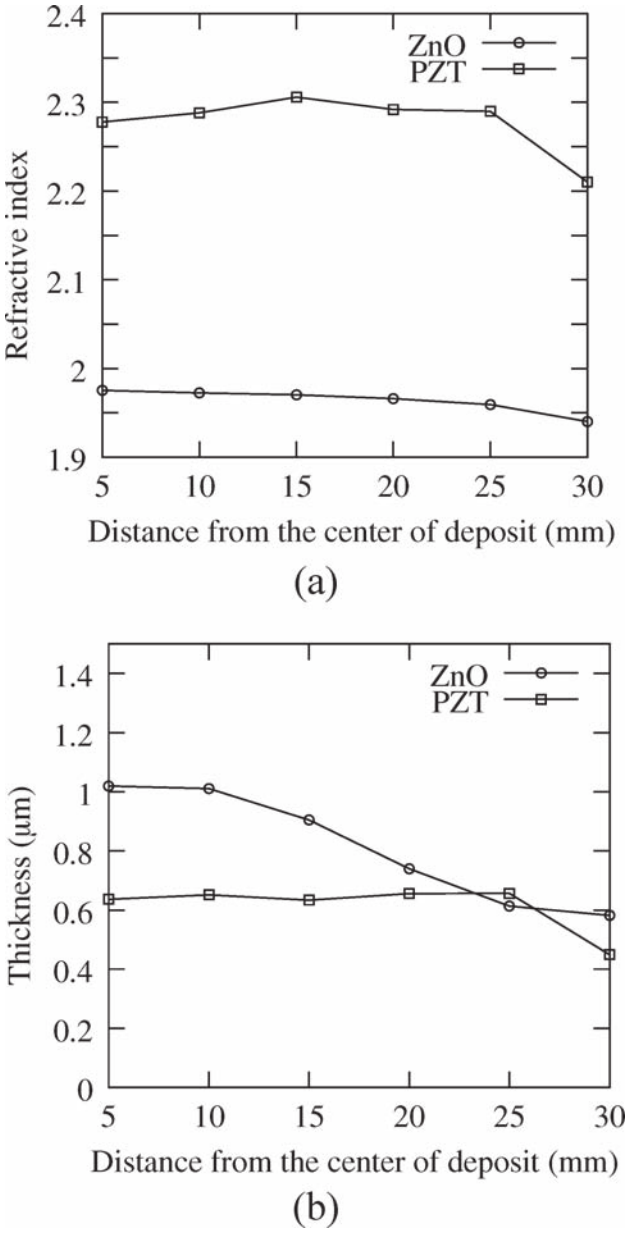

Figure 6. Evolution of the refraction index (a) and the film thickness (b) of a PZT/ZnO structure.

PZT film of the identical precursor composition, directly spin-coated on the glass substrate, has a refraction index close to 2.22 [13], whereas the refraction index of PZT deposited on ZnO is close to 2.30. XRD measurements show that the PZT 36/64 thin films deposited on glass had a rhomboedric structure, while the same composition spin-coated on ZnO had a tetragonal structure (XRD spectra not shown).

Finally, on top of the PZT/ZnO structure, a thin ($d_3 < 200$ nm) ZnO layer was deposited by rf magnetron sputtering, too. This latter has to be thinner than the light penetration depth in order allow evanescent wave coupling between the prism and the PZT film, as the refraction index of the ZnO is smaller than that of the PZT and the low order modes propagates only inside the PZT.

The obtained three layer composite wave guide structures were also characterised by m-lines spectroscopy at several points from the center of deposition with 5 mm spacing. Let us emphasize that, in order to avoid pollution at the interfaces, the three layers were deposited just one after the other, also implying that the three layer composite structure were characterized only after the final deposition and does not correspond to the sample investigated before. An example of an m-lines spectrum of a three layer waveguide is shown in Fig. 7. Compared to the two layer film (Fig. 5), the spectrum contains more peaks (due

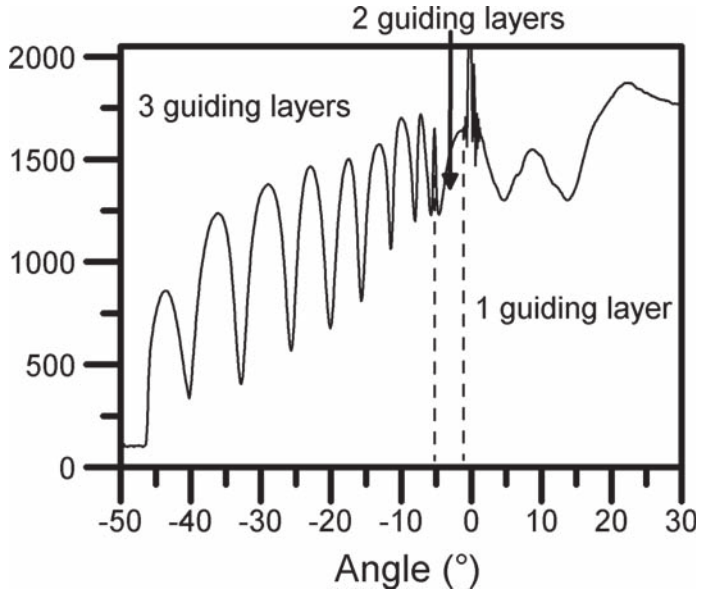

Figure 7. M-lines spectrum of a three layer ZnO/PZT/ZnO composite structure.

to a higher thickness of the bottom ZnO and the PZT film). The transition from the guiding regime in one layer to the guiding regime in two layers appears clearly in the spectrum. This is not the case for the transition from guiding regime in two layers to guiding regime in three layers. This transition has to be determined by numerical computations.

Figure 8 shows the evolution of the refraction index and the thickness of a three layer waveguide. The index of the PZT deposited on ZnO remains close to 2.3 whereas the index of PZT deposited on glass substratum is close to 2.2 [11]. These results are in agreement with those obtained by X-ray microanalysis which revealed that the PZT layers deposited on glass substratum present an excess of lead close to 40 percents whereas the PZT layers deposited on ZnO have an excess of lead close to 20 percents. The index of the bottom ZnO layer is close to 1.98, this result is in agreement with the index of ZnO two layer waveguide. The most remarkable feature is that the index of the top ZnO layer is always higher than that of the bottom layer; moreover, it exhibits relatively strong variations along the sample

Table 1
Comparison of the measured and calculated synchronous angles of a three layer waveguide

Mode order	Measured angles (°)	Calculated angles (°)	Difference
0		29.27	
1		23.61	
2		14.94	
3	3.90	3.90	$<10^{-2}$
4	−5.60	−5.60	$<10^{-2}$
5	−8.20	−8.16	4.10^{-2}
6	−11.40	−11.41	1.10^{-2}
7	−17.50	−17.43	7.10^{-2}
8	−24.80	−24.86	6.10^{-2}
9	−32.10	−32.02	8.10^{-2}

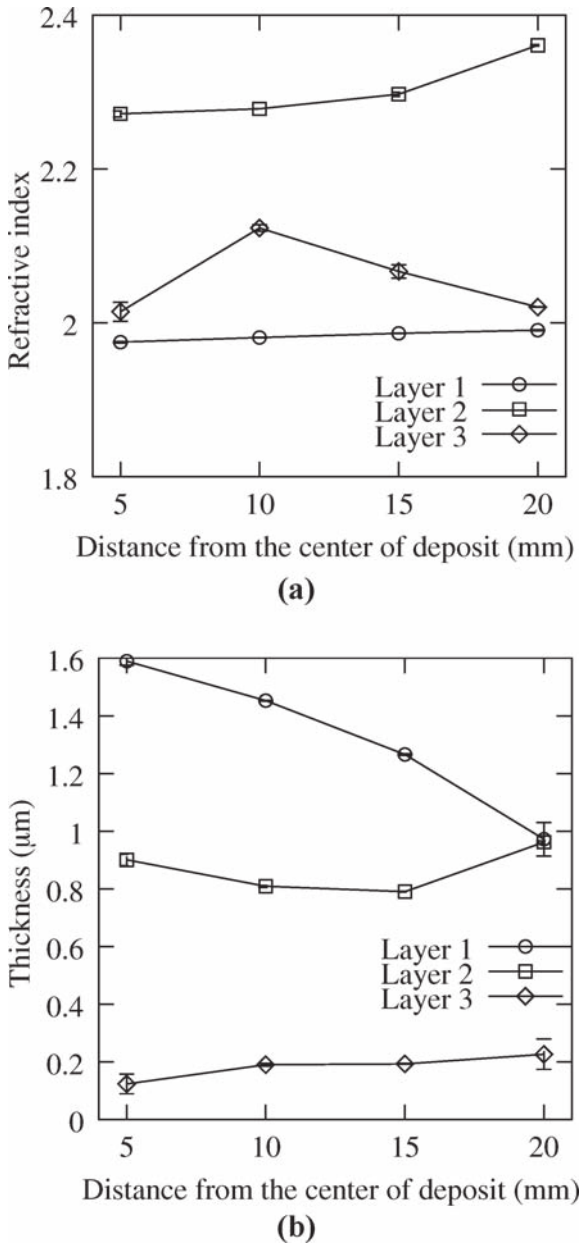

Figure 8. Evolution of the refraction index (a) and the film thickness (b) of a ZnO/PZT/ZnO composite structure.

between $n_3 = 2.02$ and $n_3 = 2.12$. This may be explained by the low thickness of this layer which is of the order of 200 nm (Fig. 8b). It is known that for a ZnO thickness below 500 nm a competition between different crystalline structures exist [14]. Hence, the top ZnO film may have a structure different from that of the bottom layer and the refraction index varies depending on which of the phases is dominating. The direction of the thickness gradient (from 120 nm to approximately 220 nm, c.f. Fig. 8b) is certainly caused by an orientation of the sample different than this during the first RF sputtering process.

In order to check the validity of our results, we used the obtained values $\{n_j, d_j\}$ as input data in order to calculate the synchronous angles with the help of equation (4). A comparison between this calculated angles ϕ^{cal} and the measured angles ϕ^{meas} is shown in Table 1, which are in very good agreement as the differences remain smaller than 0.1°. In Table 1, first guided modes were not measured because of the difficulty to excite them but the indexation criterion allows to overcome this difficulty and leads to correct solutions even if the first modes are missing. This proves the ability of the m-lines spectroscopy to accurately characterize multilayer composite waveguides.

Conclusions

A three-layer ZnO/PZT/ZnO composite waveguide structure has been elaborated by RF magnetron sputtering and Chemical Solution Deposition technique. The theoretical tools for analyzing the m-lines spectra obtained from these three-layer systems were developed and a complete determination of the refractive index and the thickness of each layer was performed. This characterization revealed the influence of the ZnO bottom layer on the PZT crystalline structure. The increase of the refraction index of the PZT deposited on ZnO compared to PZT spin-coated on glass is linked to a transition from the rhombohedral to the tetragonal structure. It also appeared that the bottom and top ZnO films did not have the same refraction index, indicating that in the thin top layer different crystalline structures may exist while only one is present in the bottom layer.

Acknowledgment

The authors wish to thank N. Barreau from the LAMP* for the deposition of the Al doped ZnO thin films.

References

1. A. Boudrioua, E. Dogheche, D. Remiens, and J. C. Loulergue. Electro-optic characterization of (Pb, La)TiO_3 thin films using prism-coupling technique. *Journal of Applied Physics* **85**, 1780–1783 (1999).
2. P. K. Tien and R. Ulrich. Theory of prism-film coupler and thin-film light guides. *Journal of the Optical Society of America* **60**, 1325–1337 (1970).
3. R. Ulrich. Theory of the prism-film coupler by plane-wave analysis. *Journal of Optical Society of America* **60**, 1337–1350 (1970).
4. R. Ulrich and R. Torge. Measurement of thin film parameters with a prism coupler. *Applied Optics* **12**, 2901–2908 (1973).
5. P. K. Tien, R. J. Martin, and G. Smolinsky. Formation of light-guiding interconnections in an integrated optical circuit by composite tapered-film coupling. *Applied Optics* **12**, 1909–1916 (1973).
6. W. Stutius and W. Streifer. Silicon nitride on silicon for optical waveguides. *Applied Optics* **16**, 3218–3222 (1977).
7. M. Matyáš, J. Bok, and T. Sikora. Determination of refractive indices and thicknesses of double-film composite waveguides. *Physica Status Solidi (a)* **126**, 533–543 (1991).
8. J. Aarnio, P. Kersten, and J. Lauckner. Determination of refractive indices and thicknesses of silica double layer slab waveguides on silicon. IEE Proc. *Optoelectron* **142**, 241–247 (1995).
9. E. Auguściuk and M. Roszko. Investigation of organic materials by generalized m-line spectroscopy method. *Proceedings of SPIE* **5451**, 495–502 (2004).
10. J. Chilwell and I. Hodgkinson. Thin-films field-transfer matrix theory of planar multilayer waveguides and reflection from prism-loaded waveguides. *Journal of the Optical Society of America A* **1**, 742–753 (1984).
11. T. Schneider, D. Leduc, J. Cardin, C. Lupi, N. Barreau, and H. W. Gundel. Optical properties of PZT thin films deposited on a ZnO buffer layer. *Optical Materials* 2006, doi:10.1016/j.optmat.2006.10.015
12. R. Seveno, P. Limousin, D. Averty, J.-L. Chartier, R. Le Bihan, and H.W. Gundel. Preparation of multi-coating PZT Thick Films by Sol-Gel Method onto Stainless Steel Substrates. *J. Europ. Ceram. Soc.* **20**, 2025–2028 (2000).

*LAMP, EA3825, Université de Nantes, Nantes Atlantique Universités, Faculté des Sciences et des Techniques, 2 rue de la Houssinière - BP 9208, Nantes, F-44000 France.

13. J. Cardin, D. Leduc, T. Schneider, C. Lupi, D. Averty, and H. W. Gundel. Optical characterization of PZT thin films for waveguide applications. *Journal of the European Ceramic Society* **25**, 2913–2916 (2005).
14. S. Lin and J. Huang. Effect of thickness on the structural and properties of ZnO films by r.f. magnetron sputtering. *Surface & Coatings Technology* **185**, 222–227 (2004).